

## A novel fast time jamming analysis transmission selection technique for radar systems

Kamal Hussein, Mohamed Mabrouk, Bahaaeldin M. F. Elsor, Ahmed Alieldin, Walid M. Saad  
Egyptian Technical Research and Development Center, Cairo, Egypt

### Article Info

#### Article history:

Received Aug 29, 2020

Revised Dec 20, 2020

Accepted Jan 19, 2021

#### Keywords:

Dual-polarized antenna  
Fast Fourier transform  
Jamming analysis transmission selection  
Jamming mitigation  
RF receiver

### ABSTRACT

The jamming analysis transmission selection (JATS) sub-system is used in radar systems to detect and avoid the jammed frequencies in the available operating bandwidth during signal transmission and reception. The available time to measure the desired frequency spectrum and select the non-jammed frequency for transmission is very limited. A novel fast time (FAT) technique that measures the channel spectrum, detects the jamming sub-band and selects the non-jammed frequency for radar system transmission in real time is proposed. A JATS sub-system has been designed, simulated, fabricated and implemented based on FAT technique to verify the idea. The novel FAT technique utilizes time-domain analysis instead of the well-known fast Fourier transform (FFT) used in conventional JATS sub-systems. Therefore, the proposed fast time jamming analysis transmission selection (FAT-JATS) sub-system outperforms other reported JATS sub-systems as it uses less FPGA resources, avoids time-delay occurred due to complex FFT calculations and enhances the real time operation. This makes the proposed technique an excellent candidate for JATS sub-systems.

*This is an open access article under the [CC BY-SA](https://creativecommons.org/licenses/by-sa/4.0/) license.*



### Corresponding Author:

Walid M. Saad  
Department of Electrical and Computer Engineering  
Egyptian Tactical Research and Development Center  
El Sayeda Aisha 11618, Cairo, Egypt  
Email: walid@sce.carleton.ca

## 1. INTRODUCTION

Wireless communication is recently one of the most important technologies of our time. It is used in different civilian, industrial, medical, military and space applications. The tremendous wireless applications enforced us to use wireless channels although they have many different impairments. Jamming is the main channel impairment in military applications. Jamming is a high-power signal generated at specific operating frequency or bandwidth to interrupt the received signal [1, 2]. That will compel the radar to operate badly in the presence of threat, which is risky. Many techniques have been used to overcome jamming from sidelobe-point of view [3, 4]. JATS is widely used in tactical surveillance radar as an effective technique to overcome the jamming effect [5].

The main function of JATS is to measure the power spectral density (PSD) across the receiver operating frequency band and reveal the undesired jammed frequencies within this band. Then it selects the best frequency within the radar frequency band that has the minimum power and uses it for radar transmission. The designs and methodologies of using JATS to determined jammed frequencies have developed a lot over the last four decades.

In [6] a surface acoustic wave device (SAW) is designed and used with an envelope detector to determine the amplitude of each frequency in the predetermined frequency band. The frequencies that have

amplitudes greater than a specific threshold are considered as jammed frequencies. The jammed frequencies are then avoided in the transmission frequency selection. The field-programmable gate array (FPGA) can be used to implement digital and analog modulation systems in modern radars [7, 8]. In [9] the FPGA is used to implement the JATS by utilizing the fast Fourier transform (FFT) core to monitor the spectrum of the channel and select either the best frequency that has minimum amplitude for transmission or the frequency agility mode with fast self-switching in real time. There are many advanced techniques to select the best single frequency or multiple frequencies in case of using frequency hopping spread spectrum [10-13].

To alleviate the FFT complexity and to enhance the time computation, the JATS is developed to calculate the average amplitude of each frequency by applying a simple algorithm using FPGA [14-17]. The JATS algorithm implemented on the FPGA determines whether the RADAR will use a fixed frequency or frequency agility mode and selects the best frequencies for RADAR transmission in a good real time.

In this paper, a novel FAT technique for JATS sub-system is proposed. The novel FAT-JATS sub-system is able to detect the jammer at very small jamming to noise ratio (JNR). Furthermore, the FPGA resources utilization is approximately 60% less. It can be utilized to countermeasure the jamming effect in pulsed radar system. The proposed system avoids the demand of high sampling rate and reduces the calculations complexity because it detects the jamming signal in time domain without monitoring the spectrum. That enhances the computation time to select the new clear non-jammed frequency for transmission in the required real time. The system is analyzed, designed, simulated and then implemented to validate the idea. The proposed system includes the design and implementation of the antenna, radio frequency (RF) receiver, the intermediate frequency (IF) receiver, and the FAT-JATS digital signal processing (DSP).

## 2. RESEARCH METHOD

The proposed FAT-JATS system is entirely designed, simulated and implemented from the antenna down to the signal processing for pulsed radar systems. It achieves lower processing time and lower hardware complexity compared to classical JATS sub-systems. The system will be presented as an antenna design, RF design, and DSP design.

### 2.1. The antenna design

To improve the signal-to-noise ratio (SNR) performance of a wireless communication system, dual polarized antennas are widely used [18, 19]. An antenna with two orthogonally polarized dipoles ensures that the polarization vector of any incident wave would be aligned with, at least, one of the receiving orthogonal dipoles [20]. So, in the proposed FAT-JATS system, a  $\pm 45^\circ$  dual-polarized cross-dipole antenna is utilized for omnidirectional coverage. The antenna consists of two elliptical-shaped crossed dipoles (Dipole A and Dipole B) printed on a square FR-4 laminate (lies in the XY plane) with a relative permittivity  $\epsilon_r=4.3$ , a loss tangent of 0.025 and a thickness of 1.6 mm as shown in Figure 1.

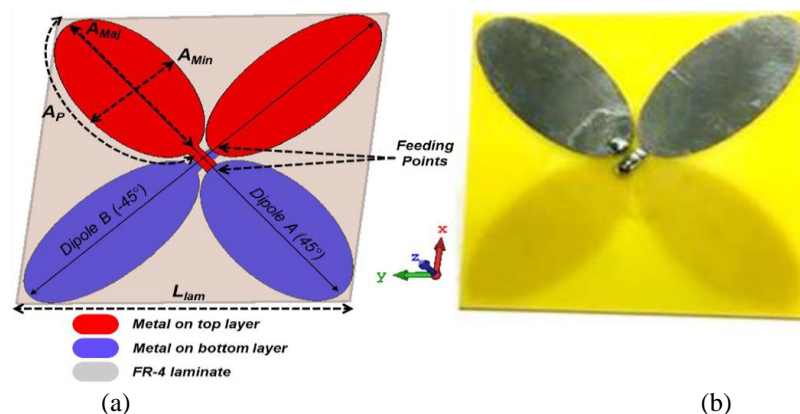


Figure 1. The proposed antenna; (a) structure (b) prototype

Dipole A consists of two elliptical elements printed on the opposite sides of the laminate. The two elements are linked by a feeding strip and an RF exciting connector. Dipole B is a rotated replica of Dipole A with a relative angle of  $90^\circ$  around Z-axis. A minor difference in Dipole B is that its feeding strip is printed

on the bottom side of the laminate to avoid intersection with the feeding strip of Dipole A. The major and minor axes of the ellipse ( $A_{Maj}$  and  $A_{Min}$  respectively) are initially chosen such that current path length across the dipole varies from  $0.5\lambda_{min}=2A_p$  to  $0.5\lambda_{max}=2A_{Maj}$ , where  $\lambda_{min}$  and  $\lambda_{max}$  are the free-space wavelengths at the start and the stop frequencies of the frequency band of interest respectively (1200 MHz and 1400 MHz in our case) and  $A_p$  is half of the perimeter of the ellipse which is linked to  $A_{Maj}$  and  $A_{Min}$  by:

$$A_p = \pi \sqrt{\frac{\left(\frac{A_{Maj}}{2}\right)^2 + \left(\frac{A_{Min}}{2}\right)^2}{2}} \tag{1}$$

The optimized dimensions of the proposed antenna can be summarized (in mm) as in Figure 1,  $A_{Maj}=48$ ,  $A_{Min}=23.5$ ,  $A_p=60$ , and  $L_{lam}=77$ . The simulated and measured S-parameters are shown in Figure 2. A good agreement between simulations and measurements can be noticed. The antenna covers the frequency band from 1200-1400 MHz with a reflection coefficient better than -15 dB ( $VSWR \leq 1.5$ ) and isolation between its ports better than -25 dB. It worth noting that both Dipole A and Dipole B have the same reflection coefficients because of the symmetry of the antenna structure. So, for simplicity, reflection coefficients of Dipole A are only presented. The antenna realized gain is shown in Figure 2. The antenna has an average realized gain of 2.2 dBi. Figure 3 presents the normalized radiation patterns at E- and H- planes ( $45^\circ$  planes) at the start, centre and stop frequencies.

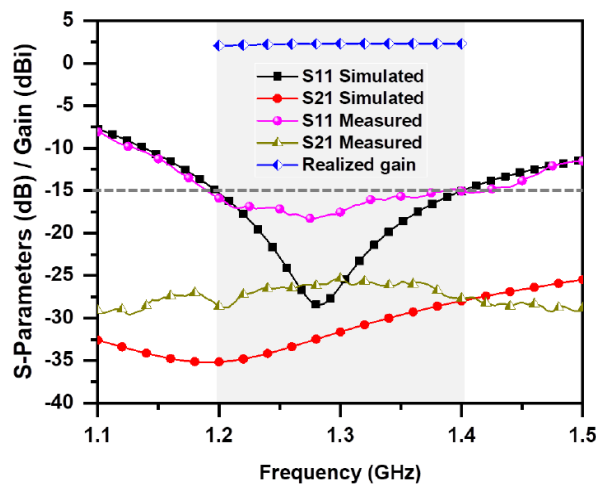


Figure 2. S-Parameters and realized gain of the proposed antenna

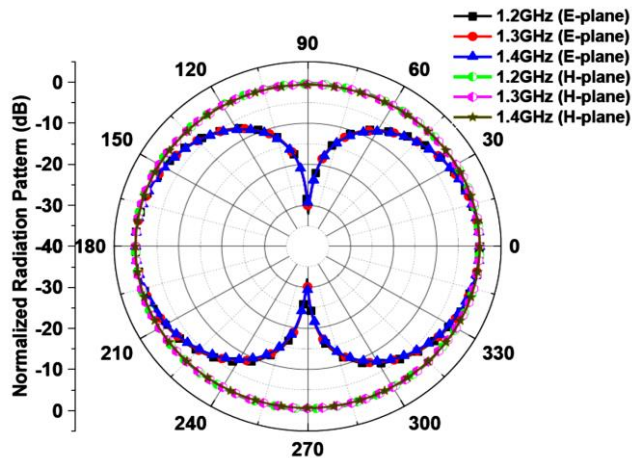


Figure 3. Normalized radiation patterns

As shown, the antenna enjoys a stable radiation pattern across the frequency band with uniform omnidirectional coverage. 3D radiation patterns at the centre frequency are presented in Figure 4 for Dipole A and Dipole B respectively. It worth noting that the received signals at the two ports are combined and then fed to the RF receiver.

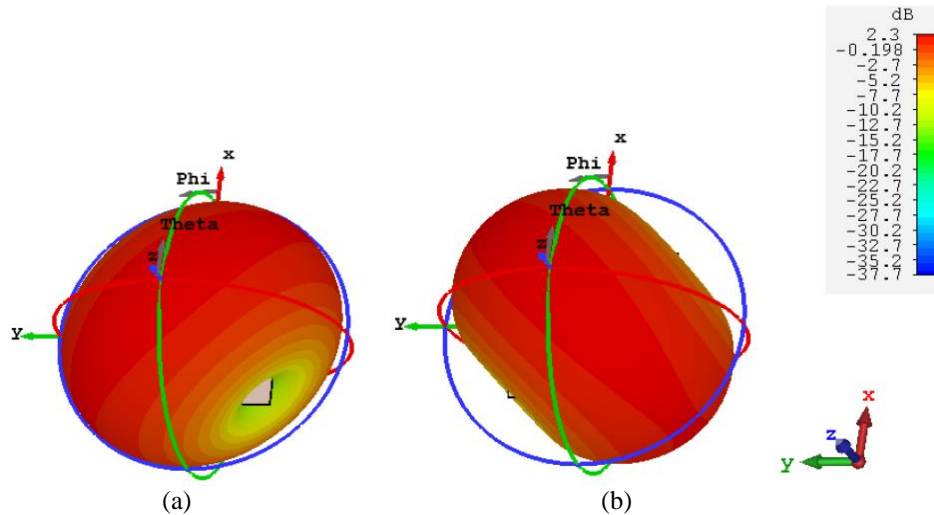


Figure 4. 3D radiation patterns of; (a) Dipole A (b) Dipole B

## 2.2. The RF design

It is necessary to detect the jamming signal that is received by the antenna. The function of the RF receiver is to enhance the sensitivity of the system to detect low power signals that may jam the main signals. In addition, it protects the used components from high power jamming signal that may saturate or degrade its operational function. This section is divided into two parts. First, the design of the RF receiver is presented and illustrated using its general block diagram. Then, the proposed RF design will be analyzed.

### 2.2.1. Principle of operation

The received RF signal with remarkable amplitude compared to the noise signal at the end of the pulse repetition time (PRT) of a pulsed radar is considered as a jamming signal [21]. As shown in Figure 5, the jamming signal is received via an RF limiter to reduce the amplitude of the jamming signal to avoid exceeding a pre-determined power limit. The first stage limiter is used to protect the low noise amplifier (LNA) from being saturated. Then a band pass filter (BPF) is used to cancel out the undesired frequencies and pass only the desired frequencies. The LNA is used to amplify the received signal to enhance the sensitivity of receiver by amplifying the noise-like jamming signal, which its amplitude is close to the noise signal (i.e.  $JNR = 0$  dB), to ease its detection. Then a second stage limiter is used to limit the power to the accepted input level of the RF input to the mixer.

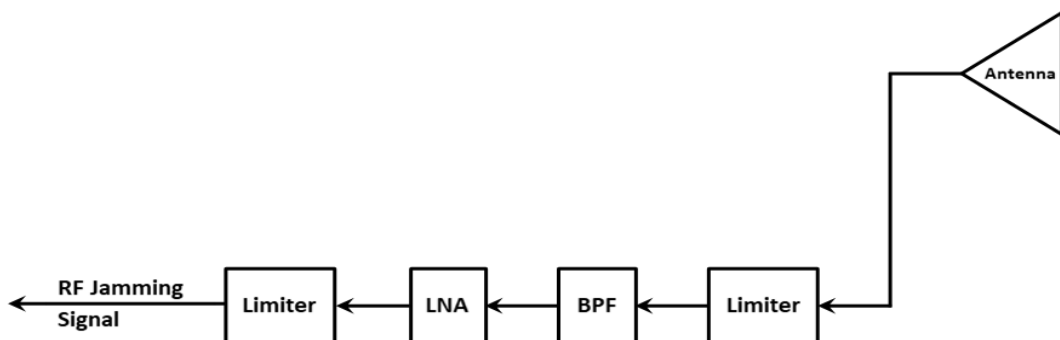


Figure 5. The RF receiver of the JATS system

### 2.2.2. Jammer signal detection model

In this section, a jammer detection mathematical model is presented. The jammer signal that is received at the front end of the antenna can be presented as (2).

$$x_j(t) = A_j e^{j(2\pi f_j t + \varphi_j(t))} \quad (2)$$

where  $x_j(t)$  is the jammer transmitted signal,  $A_j$  is the jammer transmitted signal amplitude,  $f_j$  is the jamming frequency, and  $\varphi_j(t)$  is the jammer signal phase. At the receiver, a stepped frequency modulated (SFM) signal is generated using voltage control oscillator (VCO). This signal can be presented as [22]

$$x_s(t) = A_s \cos\left(2\pi f_s t + \pi \frac{B}{T} t^2 + \varphi_s(t)\right) \quad (3)$$

where  $x_s(t)$  is the VCO generated signal,  $A_s$  is its amplitude,  $B$  is the bandwidth,  $T$  is the scan time period,  $\varphi_s(t)$  is the initial phase.  $x_s(t)$  can be represented as (4), (5).

$$\begin{aligned} x_s(t) &= A_s \cos\left(2\pi f_s t + \left(2\pi \frac{B}{2T} t\right) t + \varphi_s(t)\right) \\ &= A_s \cos\left(2\pi t \left(f_s + \frac{B}{2T} t\right) + \varphi_s(t)\right) \end{aligned} \quad (4)$$

If the two signals  $x_j(t)$  and  $x_s(t)$  are mixed at the receiver, the output signal  $x_r(t)$  can be represented as:

$$\begin{aligned} x_r(t) &= A_s \left[ \cos\left(2\pi t \left(f_s + \frac{B}{2T} t\right) + \varphi_s(t)\right) \right] \\ &\quad * A_j \left[ \cos\left(2\pi f_j t + \varphi_j(t)\right) + j \sin\left(2\pi f_j t + \varphi_j(t)\right) \right] \\ &= \frac{A_s A_j}{2} \left[ \cos\left(2\pi t \left(f_s + \frac{B}{2T} t + f_j\right) + \varphi_s(t) + \varphi_j(t)\right) \right. \\ &\quad \left. + \cos\left(2\pi t \left(f_s + \frac{B}{2T} t - f_j\right) + \varphi_s(t) - \varphi_j(t)\right) \right. \\ &\quad \left. + j \sin\left(2\pi t \left(f_s + \frac{B}{2T} t + f_j\right) + \varphi_s(t) + \varphi_j(t)\right) \right. \\ &\quad \left. + j \sin\left(2\pi t \left(f_s + \frac{B}{2T} t - f_j\right) + \varphi_s(t) - \varphi_j(t)\right) \right] \end{aligned} \quad (5)$$

Using a low-pass filter (LPF), the higher frequency will be removed and (5) can be written as:

$$\begin{aligned} x_r(t) &= A \left[ \cos\left(2\pi t \left(f_s + \frac{B}{2T} t - f_j\right) + \Delta\varphi\right) \right. \\ &\quad \left. + j \sin\left(2\pi t \left(f_s + \frac{B}{2T} t - f_j\right) + \Delta\varphi\right) \right] \end{aligned} \quad (6)$$

where  $A = \frac{A_s A_j}{2}$  and  $\Delta\varphi$  is the difference between the jammer signal phase  $\varphi_j(t)$  and the initial phase  $\varphi_s(t)$ .  $\Delta\varphi$  is an independent uniform distributed value and the amplitude  $A$  has a Rayleigh distribution [9].

Suppose that the radar system is operating across a bandwidth equal to  $B$  from a lower frequency point  $f_l$  to a higher frequency point  $f_h$ . Let  $f_s$  is equal to  $f_l$ . At some time during VCO sweep time interval  $T$ , the value of  $f_s + \frac{B}{2T} t$  will be approximately equal to  $f_j$ . This is the time that we are interested in. Assuming that the number of frequency steps generated by the VCO is 1000, then the time that we are interested in happens at one point from these 1000 points. When the mixer output  $x_r(t)$  is filtered with LPF that has a cutoff frequency equal to  $\frac{B}{1000}$ , then the amplitude of  $x_r(t)$  at this point will be:

$$x_r(t) = A [\cos(\Delta\varphi) + j \sin(\Delta\varphi)] = A e^{j\Delta\varphi} \quad (7)$$

The instant when the jammer frequency  $f_j$  is equal to the VCO frequency  $f_s + \frac{B}{2T}t$ , the signal  $x_r(t)$  will have the lowest frequency during the time interval  $T$ . If we know the time at which the lowest frequency is observed, the frequency of the jammer can be estimated based on the VCO frequency at this instant as will be illustrated in the DSP design.

### 2.3. The digital signal processing design

The general block diagram of the proposed FAT-JATS system is presented in Figure 6. The jammer signal is mixed with the VCO output that scans the bandwidth  $B$  at 1000 points during the scanning time interval  $T$ . The mixer output is filtered using a LPF with a cutoff frequency equal to 1 MHz. The filter will pass the signal  $x_r(t)$  that has the maximum amplitude at instant time  $t$  ( $\forall t \in T$ ). That happens when the jammer frequency equals to the VCO frequency (i.e.  $\Delta\varphi = 0$ ). The filter output is then digitized using 80 M. sample/second analog to digital converter (ADC). The sampled signal is then down-sampled 80 times using the FPGA board. Four main processes are implemented using the FPGA board: 10 KHz digital LPF, down sampling, peak estimation where the jammer frequency is estimated, and generating control signals for both the VCO and the radar system frequency generator.

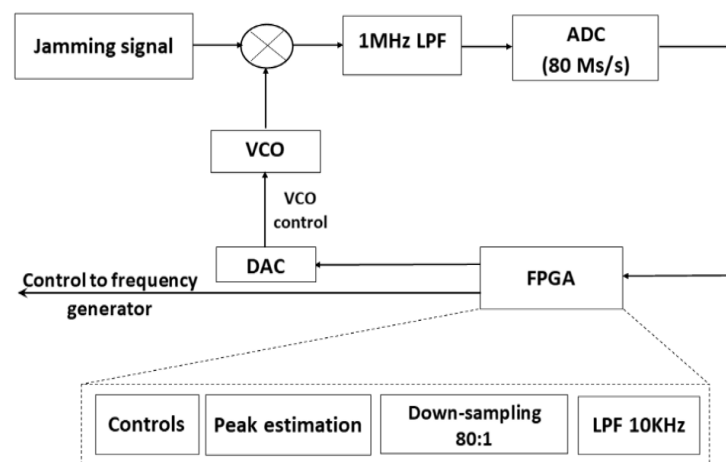


Figure 6. The general block diagram of the proposed FAT-JATS system

In the first stage of design the system is simulated using MATLAB. It is supposed that the jammer is transmitting a microwave signal with a frequency equal to 1300 MHz, and there is a communication system working in L-band from 1200 to 1400 MHz. In the following simulations, a VCO is generating 1000 step in the frequency band from 1200 to 1400 MHz, which is 200 KHz in each step. The VCO chirp time is 12.8  $\mu$ s. As given in Equation 5, the mixer output spectrum will have two main sub-bands. The first sub-band is  $f_s + \frac{B}{2T}t - f_j$ , which is [1200:1400]-1300 MHz, and the second sub-band is  $f_s + \frac{B}{2T}t + f_j$ , which is [1200:1400]+1300 MHz. The frequency spectrum of the mixer output is investigated as shown in Figure 7. It is obvious that the two sub-bands are recognized from 0:100 MHz, and from 2500:2700 MHz respectively. While mixing the VCO output and the jammer signal, the minimum output frequency response is produced when the VCO frequency becomes very close to the jammer frequency.

Consequently, the 200 KHz frequency step of the VCO gives a confident to expect that the VCO frequency output is very close to the jammer frequency  $f_j$  with 100 KHz resolution error. That means minimum produced frequency of the mixer output will be  $f_j \pm 100$  KHz. If we follow the instants when this minimal frequency is produced, then we can follow the jammer frequency. The mixer output is filtered with an FIR LPF designed using the MATLAB FDA-tool. The passband and the stopband are 1 MHz and 10 MHz respectively, with 1 dB pass amplitude, -40 dB stop amplitude and the number of coefficients is 158. Figure 8 shows the magnitude response of the 1 MHz LPF.

The filtered signal will have a maximum amplitude when the VCO frequency is equal to the jammer frequency. In Figure 9, the horizontal axis represents a single scan of the VCO. This time axis refers to an equivalent VCO frequency step at every time instant. Figure 9 shows that the maximum amplitude is obtained at the jammer frequency, which is 1300 MHz. The analog signal is then digitized using ADC with a sampling rate higher than twice the maximum frequency component in this signal. Practically, it is preferred

to sample the analog signal with a sampler that has a sampling rate more than 5 times of the highest frequency component in the signal. In this simulation, it is supposed that we have an 80 MHz ADC to sample the analog signal.

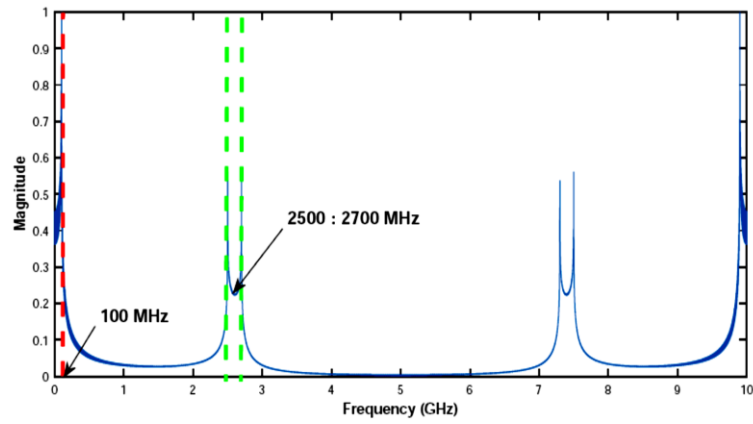


Figure 7. The spectrum of the mixer output

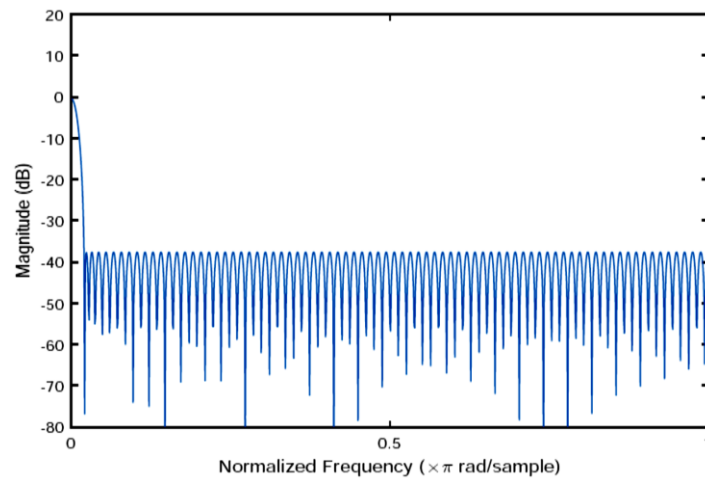


Figure 8. 1 MHz FIR LPF magnitude response

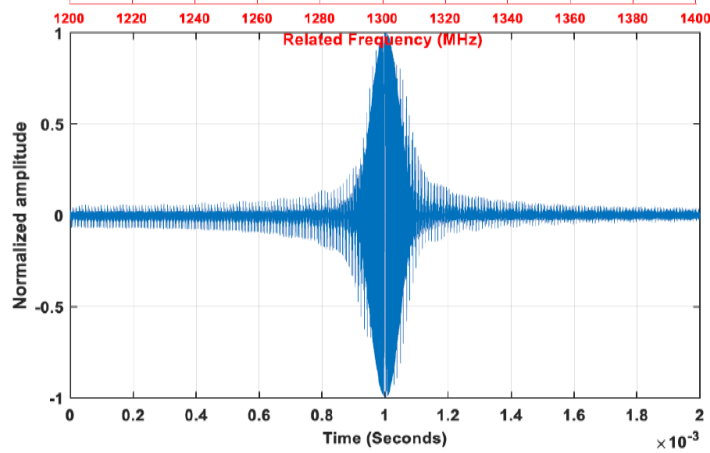


Figure 9. The 1 MHz FIR filter output signal

To enhance the resolution of the detected peaks in Figure 9, the mean of the signal is being tracked by a sliding window [23]. A moving average window with length equal to 100 samples is used to enhance the peak resolution and minimize the effect of the Gaussian noise. The output of the moving average sliding window can be presented by (8):

$$x_{MA}(n) = \frac{1}{100} \sum_{n-99}^n x(n) \quad (8)$$

where  $x(n)$  is the sampled signal and  $x_{MA}(n)$  is the output of the moving average sliding window filter. The digital signal will be processed on a processing field programmable gate array (FPGA) based board. For efficient processing time and least used resources, the digital signal is down sampled 80 times to reach a sampling rate equal to 1 MHz. Figure 10 shows the moving average sliding window filter output when the signal in Figure 9 is applied to it. The signal is down sampled with a down sampling ratio equal to 80:1.

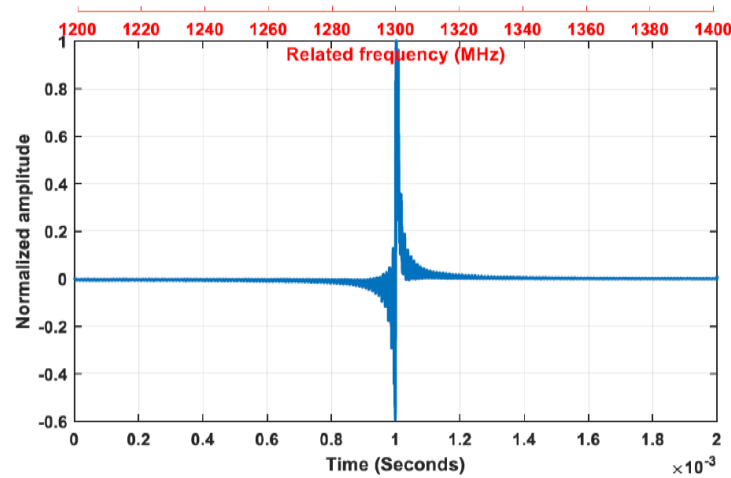


Figure 10. The moving average sliding window output for the signal  $x(n)$

The signal is then applied to a digital FIR LPF with a passband frequency equal to 10 KHz to reduce the high frequency components that was generated from intermodulation, mismatch, and cross talk between tracks on the baseboard. Figure 11 shows the filtered signal using the 10 KHz LPF. To convert the bipolar signal to a unipolar signal, the absolute value for each consequent sample are summed and divided by two. The new unipolar signal  $x_{UMA}(n)$  can be presented by (9).

$$x_{UMA}(n) = \frac{|x_{MA}(n)| + |x_{MA}(n-1)|}{2} \quad (9)$$

Figure 12 shows the proposed FAT-JATS system output when the input is a unipolar signal  $x_{UMA}(n)$ , which is 1300 MHz used as a jamming signal. To illustrate the jamming detection performance of the proposed system. A radar system is a perfect example for this proposed system. If the radar is working in the L-band from 1200 to 1400 MHz, then the worst channel to use in this case is around the 1300 MHz. Although the peak amplitude of the detected jamming signal (1302 MHz) is slightly shifted from the jammer frequency (1300 MHz), it will not affect the functionality of the FAT-JATS system. That is because the radar channels have a bandwidth, usually, not less than 5% of the whole system bandwidth. By jamming any frequency in a specific channel, all the channel will be considered jammed.

Suppose that we have three jamming signals at frequencies 1280, 1300, and 1340 MHz. The three signals are applied to the proposed algorithm. The three Jamming signals are detected at the same frequencies successfully as shown in Figure 13. It is desirable to investigate the performance of the FAT-JATS system versus the jamming-to-noise ratio (JNR). Suppose that the JNR is 0 dB, which means that the jamming power is equal to the noise power. This case is the worst case that the FAT-JATS systems may encounter. If there are three jamming signals (e.g. at frequencies 1280, 1300, and 1340 MHz), and with a JNR equal to 0 dB, the

system will still be able to detect jammed channels at these frequencies. Figure 14 shows the detected amplitude for each jamming signal using the FAT-JATS system.

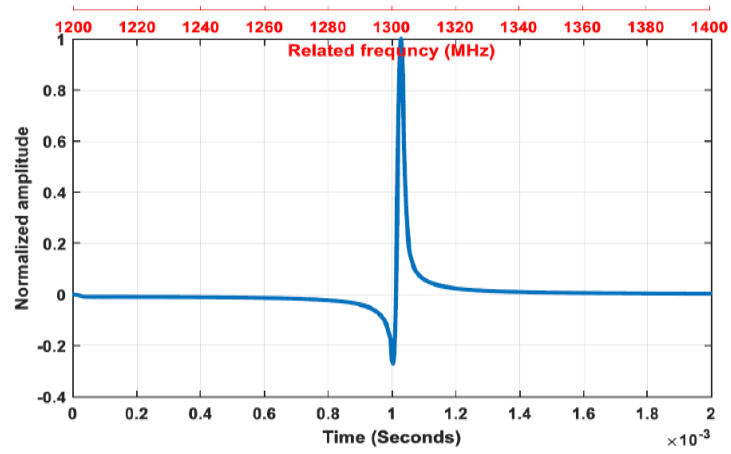


Figure 11. The filtered signal using 10 KHz LPF

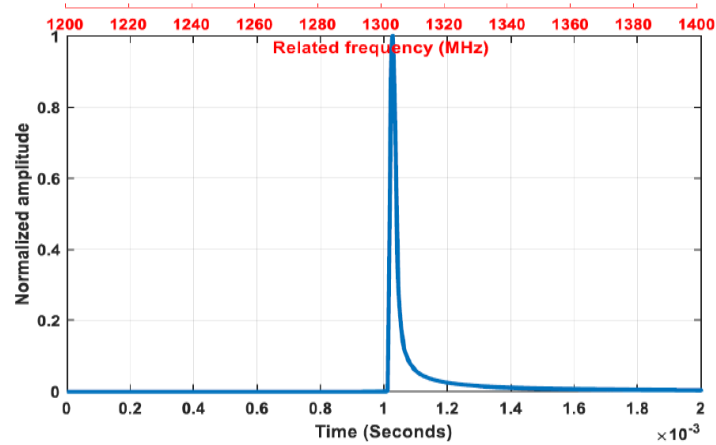


Figure 12. The FAT-JATS system output unipolar signal  $x_{UMA}(n)$

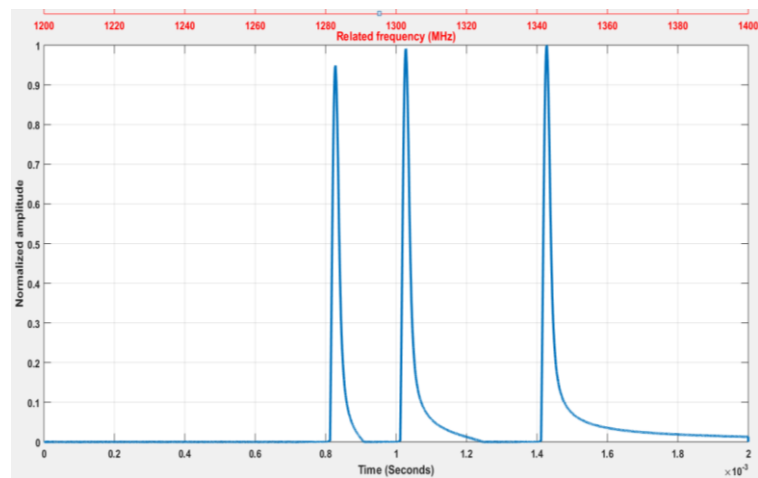


Figure 13. Three jamming signals detection at frequencies 1280, 1300, and 1340 MHz

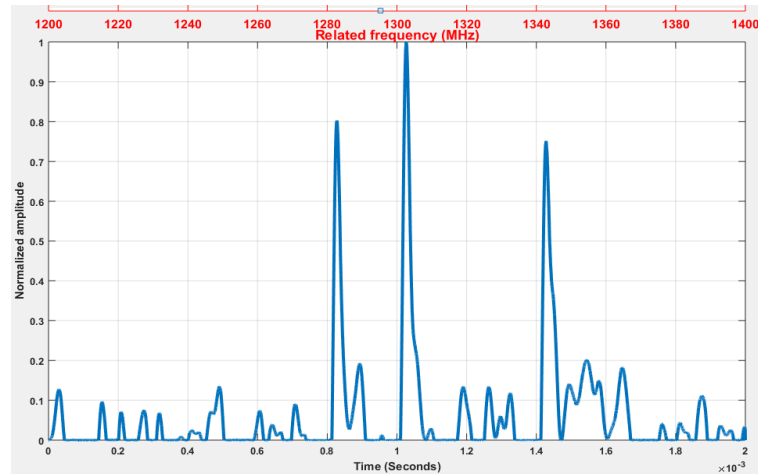


Figure 14. Three jamming signals are detected at JNR=0 dB

### 3. RESULTS AND DISCUSSION

This section illustrates an experiment that is performed to prove that the methodology and simulations are the same as the real measurements. It was assumed that the jamming signal is composed of three frequency tones 1280, 1300, and 1340 MHz. These frequencies were generated using three SLSM5-12 frequency synthesizers produced by Luff Research Company. The experiment setup was performed as shown in Figure 6. The jamming signals are mixed with the minicircuits ZX95-1750W-S+ VCO output signal using mini-circuits ZX05-C24LH-S+ RF mixer. The VCO control signal is generated using AD9280 digital-to-analog converter and Spartan 6 Xilinx FPGA. Figure 15 shows the VCO control signal. The 10-bit digital words with digital values saved in a memory were used to generate the VCO control signal producing 1024 steps which is consequently producing 1024 frequencies in the required bandwidth (1200-1400 MHz). The clock signal that is used to convert the digital word to the analog control signal is repeated every 12.5 ns, that the control signal is a sawtooth signal repeated every  $12.5 \text{ ns} \times 1024 = 12.8 \mu\text{s}$ .



Figure 15. The VCO analog control signal

The mixer analog output signal is filtered using a 1 MHz LPF then digitized using 80 MHz ADC. The digital signal is down sampled with a down sampling ration equal to 80:1 then processed on the Spartan 6 Xilinx FPGA. The processing steps are: Applying a moving average window as presented in (8), applying a 10 KHz digital LPF, converting the bipolar signal to a unipolar signal, and peak detection to estimate the jammer frequency. These steps were presented previously in section 2. Figure 16 shows the system output using ISE design suite. It is obvious that the three jammer frequencies are detected. Figures 11-13 are matched to the real implemented system output.

The experiment setup is established according to Figures 5 and 6. The jamming frequency is assumed 1300 MHz and it is generated by a keysight frequency generator model N5171B as shown in Figure 17. The FPGA is used to control the sweep time of the VCO. The ADC output is received and illustrated on a computer screen. The bandwidth (200 MHz) is divided among 16 sub-bands from 1 to 16 (i.e. each sub-band is 12.5 MHz as prescribed by the band pass filter of the filter bank). It is noticed that sub-band

number 8 is detected as a jammer, which is related to the assumed jamming frequency (1300 MHz), and it is in the center of the operating bandwidth. Once the jamming sub-band is detected, a different sub-band with good channel characteristics will be selected to be used by the radar transmitter.

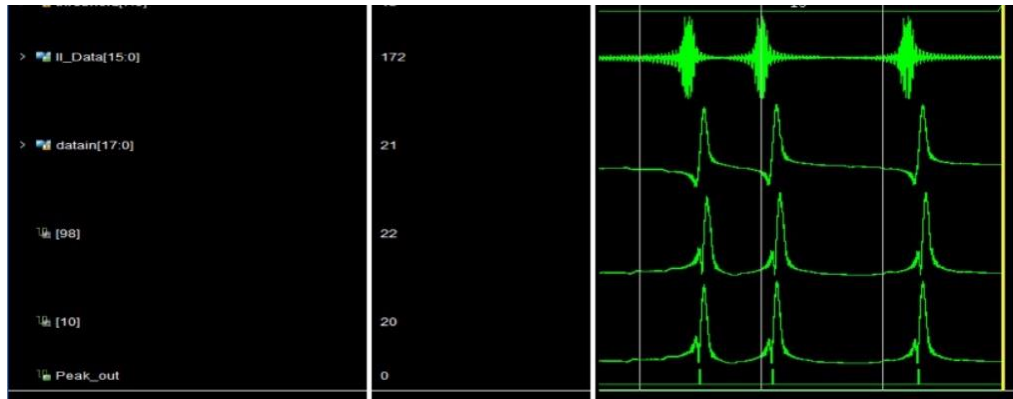


Figure 16. The system output using ISE design suite

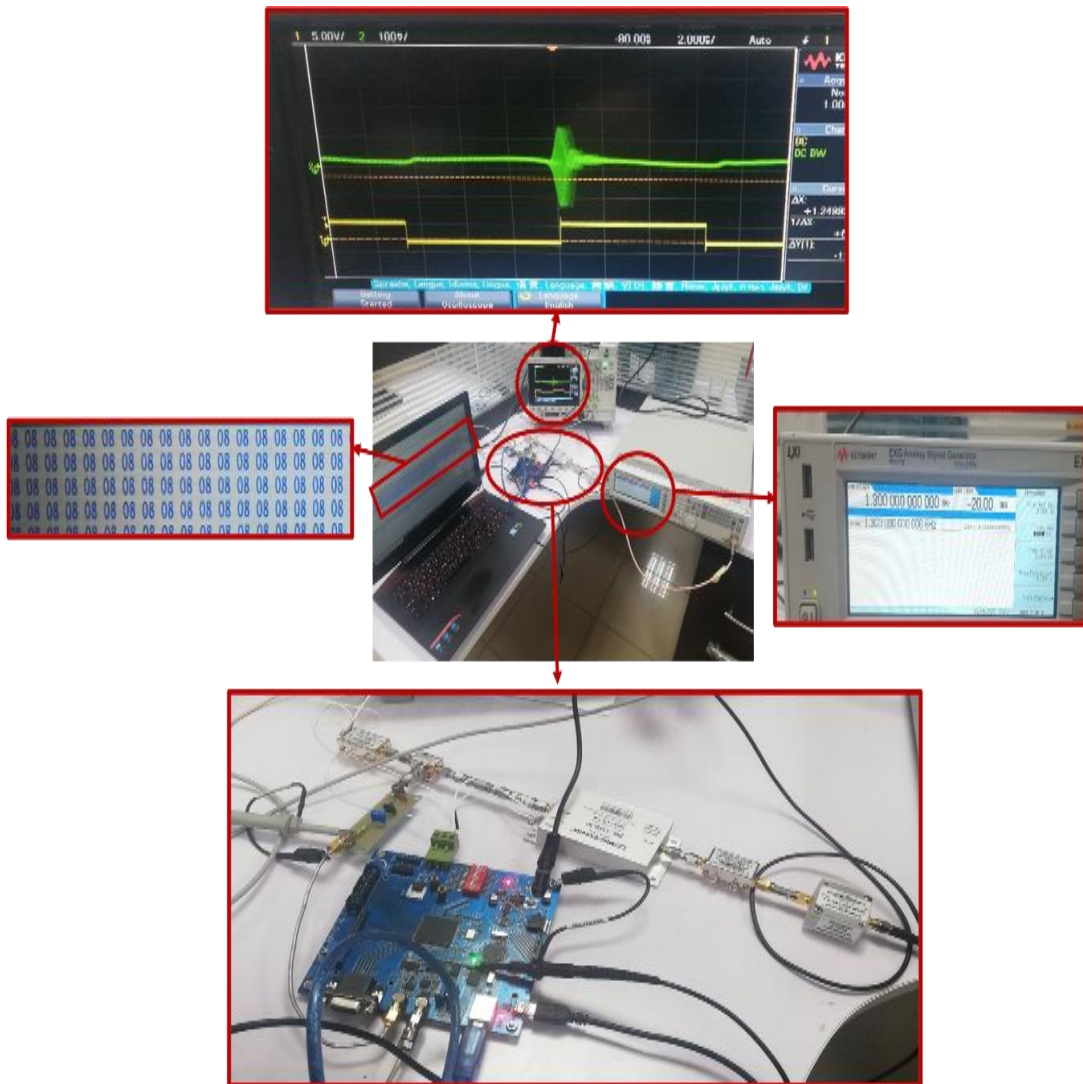


Figure 17. The experiment setup

A comparison between the proposed FAT-JATS technique and the traditional FFT method [24, 25] is presented in this section from FPGA resources utilization point of view. The design is implemented for both methods on the Xilinx SPARTAN6 XC6SLX9-2tqg144. Table 1 shows the device utilization for both FAT-JATS technique and the traditional FFT method. The traditional FFT method consumes nearly three times the resources of the proposed FAT-JATS technique.

Table 1. FPGA utilization for both FFT and FAT-JATS techniques

Hardware resources	Available resources	FFT technique	Proposed FAT technique
slice LUTs	5720	673 (12%)	212 (4%)
flip flops	11440	219 (2%)	120 (1%)
bonded IOBs	102	30 (30%)	30 (30%)
number used as BUFs	16	4 (25%)	4 (25%)
DSP slices	16	11 (70%)	0 (0%)
LUT RAM	245	35 (15%)	33 (14%)
block RAM	576 kb	151 (26%)	0 (0%)

#### 4. CONCLUSION

The paper has proposed a complete design, simulation and implementation for a developed FAT-JATS system to mitigate jamming in real time for radar systems. The conventional FFT method that is implemented on the same FPGA board to estimate the frequency spectrum of the operational bandwidth and to select the new non-jammed operating frequency utilizes approximately three more times resources than the proposed method. Furthermore, to implement the FFT method to achieve jamming analysis for the entire operating bandwidth (i.e. 200 MHz), we need a higher sampling rate ADC, which is practically five times the operating bandwidth (i.e. 1 GS). Otherwise, in the proposed method we just need an ADC with sampling rate not more than 10 M samples/sec because the interested bandwidth is less than 2 MHz after the sweep down conversion. The proposed FAT-JATS technique is able to detect the jamming sub-band and refresh the jamming detection every one full sawtooth signal (12.8  $\mu$ s). That allows the radar system to change the operating frequency from pulse-to-pulse during the dead time without any time delay. To conclude, the proposed FAT-JATS system improves the complexity caused by the FFT methods, uses less FPGA resources and support the radar system to operate in real time.

#### REFERENCES

- [1] S. L. M. Hassan, N. Sulaiman, S. S. Shariffudin, T. N. T. Yaakub, "Signal-to-noise Ratio Study on Pipelined Fast Fourier Transform Processor," *Bulletin of Electrical Engineering and Informatics (BEEI)*, vol. 7, no. 2, pp. 230-235, Jun. 2018, doi: 10.11591/eei.v7i2.1167.
- [2] J. Schuerger, D. Garmatyuk, "Deception Jamming Modeling in Radar Sensor Networks," *Military Communications Conference (MILCOM)*, San Diego, CA, Nov. 2008, pp. 1-7, doi: 10.1109/MILCOM.2008.4753118.
- [3] J. R. Mohammed and K. H. Sayidmarie, "Performance Evaluation of the Adaptive Sidelobe Canceller with various Auxiliary Configurations," *AEU International Journal of Electronics and Communications*, vol. 80, pp. 179–185, Oct. 2017, doi: 10.1016/j.aeu.2017.06.039.
- [4] J. R. Mohammed and K. H. Sayidmarie, "A New Technique for Obtaining Wide-Angular Nulling in the Sum and Difference Patterns of Monopulse Antenna," *IEEE Antennas and Wireless Propagation Letters*, vol. 11, pp. 1245-1248, Oct. 2012, doi: 10.1109/LAWP.2012.2224086.
- [5] Jossef, A., Davidson, R. Y., Levin, R., and Hect, I., "Method and apparatus for signal detection and jamming," U.S. Patent No. 7,023,374, 2002.
- [6] C R. Vale, "Method and System for Jamming Analysis and Transmission Selection," United States Patent US4328497A, May 4, 1982.
- [7] R. K. Mohammed and H. A. Abdullah, "Implementation of Digital and Analog Modulation Systems Using FPGA," *Indonesian Journal of Electrical Engineering and Computer Science*, vol. 18, no. 1, pp. 485-493, 2020.
- [8] R. Taniza, K. Jadia, G. S. N. Raju, M. Chandramohan, "High density FPGA based waveform generation for radars," *2010 IEEE Radar Conference*, Washington, DC, USA, May 2010, pp. 310-314.
- [9] T. Pechetty and R. Udumudi, "FPGA Implementation of Interference Avoidance and Hard To Intercept Frequency Agile Radar Processing," *International Journal of Soft Computing and Engineering (IJSCE)*, vol. 2, no. 3, pp. 207-212, Jul. 2012.
- [10] S. E. El-Khany and W. M. Saad, "New Technique for Enhancing the Signaling in Slowly Fading Dispersive Channels," *5<sup>th</sup> Intl. Conf. on Wireless Commun., Networking and Mobile Computing (WiCom)*, 2009, pp. 1-4.
- [11] A. K. Aboul-Seoud, M. El-Barbry, and A. S. Haféz, "Radar ECCM Techniques Implementation Using Microcontrollers," *21<sup>st</sup> International Conference on Computer Theory and Applications (ICCTA)*, 2011.
- [12] W. M. Saad and I. Marsland, "Jamming and Fading Channels Mitigation Using Anti-jamming Advanced Frequency Hopping," *International Conference on Electrical and Computer Systems*, Ottawa, Aug. 2012.

- [13] A. E. Mansour, W. M. Saad, S. H. El Ramly, "Adaptive Chaotic Frequency Hoping," *IEEE 10<sup>th</sup> Int. Conference on Computer Engineering & Systems (ICCES)*, Egypt, Dec. 2015, pp. 328-331.
- [14] H. Zhou and L. Guo, "Self-adaptive Frequency Agility Realized with FPGA," *IEEE International Conference on Image Analysis and Signal Processing*, China, April 2009, pp. 419-422.
- [15] A. Kumar, B. Singh, J Manasa, Y. Sravani and B. Saraswathi, "Frequency Agile Radar Processing Unit Realized with FPGA," *International Journal of Scientific & Technology Research (IJSTR)*, vol. 1, pp. 48-50, Nov. 2012.
- [16] K. Praveena and C. Priya, "Fast Self Switching Type Frequency Agile RADAR Processing Unit Implemented on Xilinx FPGA," *International Journal of Engineering Research and Applications (IJERA)*, vol. 3, pp. 1459-1462, Apr. 2013.
- [17] K. Lakshmi and K. Reddy, "Implementation of High Speed Self Switching Frequency Agile RADAR," *International Journal of Computer Science and Technology (IJCT)*, vol. 4, pp. 262-266, Dec. 2013.
- [18] X. P. Mao and J. W. Mark, "On Polarization Diversity in Mobile Communications," *International Conference on Communication Technology*, Guilin, Nov. 2006, pp. 1-4.
- [19] M. Stanley, Yi Huang, H. Wang, H. Zhou, A. Alieldin and S. Joseph *et al.*, "A Dual-Band Dual-Polarised Stacked Patch Antenna for 28 GHz and 39 GHz 5G Millimetre-Wave Communication," *13<sup>th</sup> European Conference on Antennas and Propagation (EuCAP)*, 2019, pp. 1-4.
- [20] A. Alieldin and Y. Huang, "Design of Broadband Dual-polarized Oval-shaped Base Station Antennas for Mobile Systems," *IEEE International Symposium on Antennas and Propagation & USNC/URSI National Radio Science Meeting*, San Diego, CA, Jul, pp. 183-184, 2017, doi: 10.1109/APUSNCURSINRSM.2017.8072134.
- [21] M. I. Skolnic, "Radar Handbook," MC Graw Hill, 2<sup>nd</sup> edition, Chapter 3, Apr. 1990.
- [22] A. Ahmad, J. Roh, D. Wang and A. Dube, "Vital Signs Monitoring of Multiple People Using a FMCW Millimeter-Wave Sensor," *IEEE Radar Conference (RadarConf18)*, Oklahoma, Apr. 2018, pp. 1450-1455.
- [23] A.G. Yarovoy, L.P. Ligthart, J. Matuzas and B. Levitas, "UWB Radar for Human Being Detection," *IEEE Aerospace and Electronic Systems Magazine*, vol. 21, no. 3, pp. 10-14, Nov. 2006.
- [24] C. B. Lim and M. H. Salih, "Design and Implementation of Embedded Concurrent Laser Missile Jammer System Using FPGA," *Indonesian Journal of Electrical Engineering and Computer Science (IJECS)*, vol. 14, no. 2, pp. 780-787, May 2019.
- [25] Md. Z. Hussain and K. N. Parvin, "Low power and high performance FFT with different radices," *International Journal of Reconfigurable and Embedded Systems (IJRES)*, vol. 8, no. 2, pp. 99-106, Jul. 2019.

## BIOGRAPHIES OF AUTHORS



**Kamal Hussein** received the B.S. degree in electrical engineering from the University of Alexandria, Alexandria, EGYPT, in 2014. He is currently an Assistant Researcher at Electronics Department, ADTRC, Egypt, and aiming for getting a M.Sc. degree from Ain Shams University. His current research interests include Software Defined Radio, High-speed circuits Design, Radar applications.



**Mohamed Mabrouk** received his BSc. degree in electrical and communication engineering in Alexandria University, Alexandria, Egypt in 1998. He received M.Sc. degree from the same university in electrical and communication engineering in 2009. Since this time, he was interested in radar system design and data processing. In 2015, he received his PhD in University of Ottawa, Ottawa, Canada. During his PhD research, he worked on human breathing and heartbeat rate estimation in free space or behind the wall. He works in biomedical signal analysis, biomedical signal processing, digital signal processing, DOA estimation, jamming suppression, and radar signal processing fields. Recently, he is a system engineer in designing and implementing radar systems.



**Bahaaeldin M. F. Elsor** received the B.S. degree in electrical engineering from the University of Alexandria, Alexandria, EGYPT, in 2005. Obtain M.sc degree at 2016. He is currently an Assistant Researcher at Electronics Department, A.D.R&D Center, Egypt, and aiming for getting a PHD. degree. His current research interests include Digital signal processing, Real-time processing applications, Radar applications.



**Ahmed Alieldin** received the B.Sc. degree in radar engineering from the Military Technical College, Egypt, in 2005, the M.Sc. (Eng.) degree in antenna and microwave Propagation from the University of Alexandria, Egypt, in 2013, and the Ph.D. degree in antennas and electromagnetics from the University of Liverpool, U.K., in 2019. His academic research activities and Ph.D. were centred on antenna designing and measurements with an emphasis on mobile communication applications. In addition to work in academia, he also held various positions throughout more than ten years working in the industry. He is currently a Senior RF Research Scientist with The Egyptian Technical Research and Development Centre. His current research interests include novel textile antennas, multiple-input multiple-output antennas, base station antennas, satellite antennas, transparent antennas, high power antenna, phased-MIMO radar antennas and various types of RF and microwave circuits.



**Walid M. Saad** was born in Alexandria, Egypt. He received a B. Sc. degree in Electrical Engineering in 1999 from the Air Defence College, Alexandria University, M.S. degree in Electrical Engineering in 2009 from Alexandria University, Alexandria, Egypt and Ph.D degree in systems and computer engineering in 2014 from Carlton University, Ottawa, Canada. He is currently a visitor lecturer in Egyptian Air Defence College (ADC). He is also the chief of microwave department in the Egyptian Air Defence Technical Research and Development Center (ADTRC). Recently he is the manager of the Egyptian Radar Research Center (ERRC).